



The Black Hole Mass of Abell 1836-BCG and Abell 3565-BCG

E. Dalla Bontà^{1,2}, L. Ferrarese², E. M. Corsini¹, J. Miralda-Escudé³, L. Coccato⁴,
and A. Pizzella¹

¹ Dipartimento di Astronomia, Università degli Studi di Padova, Vicolo dell'Osservatorio,
3, I-35122 Padova, Italy, e-mail: elena.dallabonta@unipd.it

² Herzberg Institute of Astrophysics, Victoria, Canada

³ Institut de Ciències de l'Espai (CSIC-IEEC)/ICREA, Bellaterra, Spain

⁴ Max-Planck-Institut fuer extraterrestrische Physik, Garching bei Muenchen, Germany

Abstract. Two brightest cluster galaxies (BCGs), namely Abell 1836-BCG and Abell 3565-BCG, were observed with the Advanced Camera for Surveys (ACS) and the Space Telescope Imaging Spectrograph (STIS) on board the Hubble Space Telescope. By modeling the available photometric and kinematic data, it resulted that the mass of Abell 1836-BCG and Abell 3565-BCG are $M_{\bullet} = 4.8^{+0.8}_{-0.7} \times 10^9 M_{\odot}$ and $M_{\bullet} = 1.3^{+0.3}_{-0.4} \times 10^9 M_{\odot}$ at 1σ confidence level, respectively.

Key words. black hole physics, galaxies: kinematics and dynamics, galaxies: structure

1. Introduction

Many nearby galaxies have revealed large dark masses in small regions, so far explained only in terms of supermassive black holes (SBHs, see for a review Ferrarese & Ford 2005). Spectroscopic and photometric data at high spatial resolution have made it possible to derive relatively accurate SBH masses, M_{\bullet} , for a number of galaxies. These measurements are reliable if the SBH sphere of influence is solved. It was also found that M_{\bullet} correlates with other galaxy properties, such as bulge luminosity (Magorrian et al. 1998, Marconi & Hunt 2003), light concentration (Graham et al. 2001), and bulge velocity dispersion σ (Ferrarese & Merritt 2000; Gebhardt et al. 2000). The inextricable link between the evo-

lution of SBHs and the hierarchical build-up of galaxies is most directly probed by the systems that have undergone the most extensive and protracted history of merging, namely the massive galaxies associated with the largest SBHs. This is the case of brightest cluster galaxies (BCGs). Their large masses and luminosities, as well as their having a merging history which is unmatched by galaxies in less crowded environments, make BCGs the most promising hosts of the most massive SBHs in the local Universe. Therefore from Laine et al. (2003) it was selected a sample of BCGs, predicted to host the most massive SBHs (based on the $M_{\bullet} - \sigma$ and $M_{\bullet} - M_B$ relations), and for which the SBH sphere of influence could be well resolved using the $0''.1$ wide slit of Space Telescope Imaging Spectrograph (STIS) on board the Hubble Space Telescope (HST).

Send offprint requests to: E. Dalla Bontà

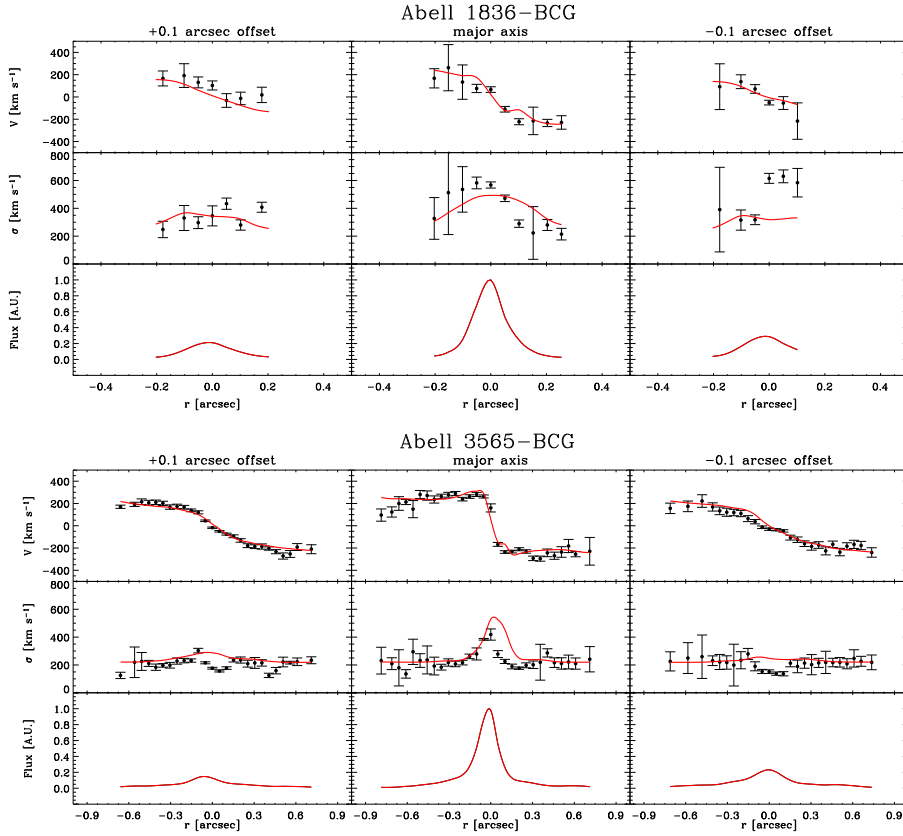


Fig. 1. Observed [N II] $\lambda 6583$ kinematics (filled circles) along with the best-fitting model (solid line) for the SBH mass of Abell 1836-BCG and Abell 3565-BCG. The observed and modeled velocity curve (top panels) and velocity dispersion radial profile (central panels) are shown for the slit along the major axis (central panels), and the two offset positions (left and right panels) of the gas disk. The corresponding modeled flux profile is shown in the bottom panels.

2. Imaging and spectroscopy

Abell 1836-BCG and Abell 3565-BCG were observed with three filters of the Advanced Camera for Surveys (ACS): F435W (which resembles the Johnson B filter), F625W (similar to r in the Sloan Digital Sky Survey photometric system), and the narrow-band (≈ 130 Å) ramp filter FR656N, covering the redshifted $H\alpha$ and [N II] $\lambda\lambda 6548, 6583$ emission lines in the nucleus of each galaxy. The images were used to determine the optical depth of the dust, stellar mass distribution near the nucleus, and intensity map. Besides, high-resolution spectroscopy of the $H\alpha$ and [N II] $\lambda 6583$ emission

lines was obtained for both galaxies, to measure the central ionized-gas kinematics. A major axis spectrum was obtained with the slit crossing the nucleus of the galaxy. Two additional offset spectra were obtained displacing the slit by one slit width on either side, perpendicularly to the slit axis. Ionized-gas kinematics was measured by fitting position, width, and flux of the [N II] $\lambda 6583$ line. Figs. 1 and 2 show the kinematics of Abell 1836-BCG and Abell 3565-BCG, respectively. They reveal regular rotation curves and strong central velocity gradients, thus they are good candidates for dynamical modeling.

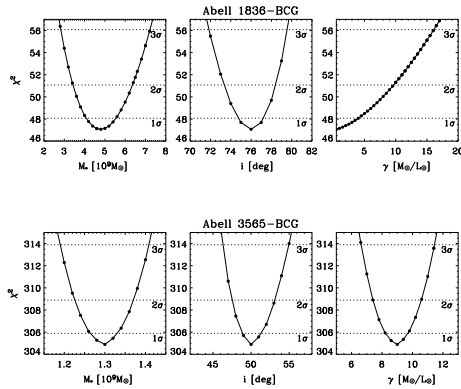


Fig. 2. χ^2 distribution for Abell 1836-BCG (*top panels*) and Abell 3565-BCG (*bottom panels*) as a function of SBH mass (*left panel*), inclination (*central panel*), and stellar mass-to-light ratio (*right panel*). The dotted horizontal lines indicate the confidence levels on the best fitting values.

3. Dynamical modeling

For this study, the procedure described in Coccato et al. 2006, to which the reader is referred for details, was followed to model the ionized-gas kinematics. Briefly, a synthetic velocity field was generated assuming that the ionized gas is moving in circular orbits in an infinitesimally thin disk centered at the nuclear location, under the combined gravitational potential of stars and SBH. The model is projected onto the plane of the sky for a given inclination of the gaseous disk, and then degraded to simulate the actual setup of the spectroscopic observations. The latter step includes accounting for width and location (namely position angle and offset with respect to the center) of each slit, STIS PSF, and charge bleeding between adjacent CCD pixels. The free parameters of the model are the mass M_\bullet of the SBH, mass-to-light ratio $(M/L)_\star$ of the stellar component (and dark matter halo), and inclination i of the gaseous disk. Both $(M/L)_\star$ and i are assumed to be radially invariant. Although i can be estimated from the images of the disk, the ionized gas is concentrated in the innermost region of the dust disk and slight warps can be present even in the case of disks with a

regular elliptical outline (e.g., Ferrarese et al. 1996; Sarzi et al. 2001; Shapiro et al. 2006). Therefore i is best treated as a free parameter. The surface brightness distribution of the ionized gas is treated as input, by the narrow-band imaging. The velocity dispersion of the emission lines was assumed to be described by the radial function $\sigma(r) = \sigma_0 + \sigma_1 e^{-r/r_\sigma}$, with the choice of the best parameters to reproduce the observables. M_\bullet , $(M/L)_\star$, and i were determined by finding the model parameters which produce the best match to the observed velocity curve, obtained by minimizing $\chi^2 = \sum (v - v_{mod})^2 / \delta^2(v)$ where $v \pm \delta(v)$ and v_{mod} are the observed and the corresponding model velocity along the different slit positions, respectively.

4. Results

For Abell 1836-BCG a three-dimensional grid of models was explored, with $0 \leq M_\bullet \leq 3.0 \times 10^{10} M_\odot$ in $2.0 \times 10^8 M_\odot$ steps, $0^\circ \leq i \leq 90^\circ$ in 1° steps, and $0 \leq (M/L)_\star \leq 40 (M/L)_\odot$ in $0.5 (M/L)_\odot$ steps. The best model fitting the observed rotation curve requires $M_\bullet = 4.8^{+0.8}_{-0.7} \times 10^9 M_\odot$, $i = 76 \pm 1^\circ$, and $(M/L)_\star \leq 4.0 (M/L)_\odot$, where the errors on M_\bullet and i , and the upper limit on $(M/L)_\star$, are quoted at the 1σ confidence level. This is the largest SBH mass to have been dynamically measured to date. The model is compared to the observed [N II] $\lambda 6583$ kinematics in Fig. 1. Figure 2 shows 1σ , 2σ , and 3σ confidence levels individually on M_\bullet , i , and $(M/L)_\star$, according to the $\Delta\chi^2$ variations expected for one parameter, with the other two held fixed at their best-fitting values.

The rotation curves of Abell 3565-BCG along the three slit positions were fitted for a grid of model parameters defined by $0 \leq M_\bullet \leq 5.0 \times 10^9 M_\odot$ in $2.0 \times 10^7 M_\odot$ steps, $0^\circ \leq i \leq 90^\circ$ in 1° steps, and $0 \leq (M/L)_\star \leq 15 (M/L)_\odot$ in $0.4 (M/L)_\odot$ steps. The best model requires $M_\bullet = 1.3^{+0.3}_{-0.4} \times 10^9 M_\odot$, $i = 50 \pm 1^\circ$ and $(M/L)_\star = 9.0 \pm 0.8 (M/L)_\odot$, where all errors are given at the 1σ confidence level. The model is compared to the observed kinematics in Fig. 1. Fig. 2 shows the confidence levels on M_\bullet , i , and $(M/L)_\star$ alone.

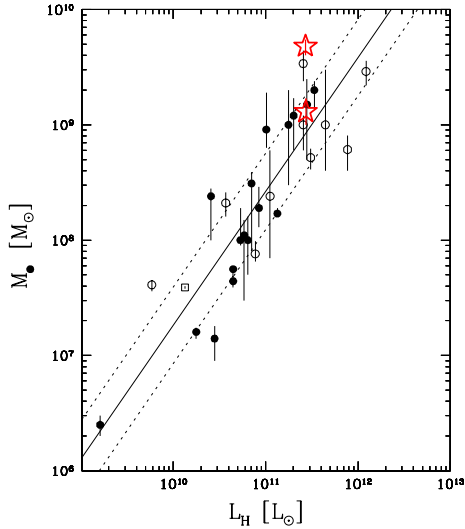


Fig. 3. Location of the SBHs masses of our BCGs (stars) with respect to the near-infrared $M_{\bullet}-L_{bulge}$ relation by Marconi & Hunt (2003). NGC 1399 was added (Houghton et al. 2006). The SBH masses based on resolved dynamical studies of ionized gas (open circles), water masers (open squares), and stars (filled circles) are plotted. Dotted lines represent the 1σ scatter of the relation.

5. Conclusions

Several authors have recently focused their attention on the position of BCGs and massive galaxies in the upper end of the SBH scaling relations, using both theoretical and, even if indirect, observational considerations. Bernardi et al. (2007) found that BCGs define a shallower $\sigma - \mathcal{L}$ relation than the bulk of early-type galaxies. They interpreted it as due to a non-linear correlation between $\log M_{\bullet}$ and $\log \sigma$. This would bring the $M_{\bullet}-\sigma$ to underestimate M_{\bullet} for high σ values. Furthermore, according to von der Linden et al. (2007) BCGs follow a steeper Faber-Jackson relation than non-BCGs. This implies that BCGs can follow at most one of the power-law relations, either the $M_{\bullet}-\sigma$ or the $M_{\bullet}-L$. Both Bernardi et al. (2007) and von der Linden et al. (2007) used SDSS data. On the contrary, Batcheldor et al. (2007) argue that SBHs masses predicted from NIR luminosities are consistent with masses

predicted from σ . They attributed the discrepancies to the presence of extended blue envelopes around the BCGs.

In order to compare the SBH mass determinations of Abell 1836-BCG and Abell 3565-BCG with the prediction of the near-infrared $M_{\bullet}-L_{bulge}$ relation by Marconi & Hunt (2003) the 2MASS H -band luminosities of the two BCGs were retrieved from the NASA/IPAC Infrared Science Archive. Figure 3 shows the location of the SBH masses in the $M_{\bullet}-L_{bulge}$ plane. Only the SBH mass of Abell 1836-BCG is not consistent with the relation, since it is larger than the one expected (i.e., $8.9 \times 10^8 M_{\odot}$). The same is true only for M 87, among the seven galaxies with $M_{\bullet} > 10^9 M_{\odot}$ dynamically measured so far. The σ of Abell 1836-BCG is not available in literature, thus it is not possible to discuss its behavior in the $M_{\bullet}-\sigma$ relation. On the other hand, all the galaxies with $M_{\bullet} > 10^9 M_{\odot}$ lie on the relation. There is no strong evidence that the upper end of the scaling relations is regulated by a different law.

The only way to hush-up the debate is adding new M_{\bullet} . Before the advent of new classes of telescopes from earth and space, adaptive optics is a viable solution (e.g., Houghton et al. 2006). It will be possible to understand the behavior of both $M_{\bullet}-\sigma$ and $M_{\bullet}-\mathcal{L}$ relations and, in case, if BCGs and normal galaxies have a bimodal trend.

References

- Batcheldor, D., et al. 2007, ApJ in press
- Bernardi, M., et al. 2007, AJ, 133, 1741
- Coccatto, L. et al. 2006, MNRAS, 366, 1050
- Ferrarese, L. et al. 1996, ApJ, 470, 444
- Ferrarese, L., Ford, H. 2005, SSRv, 116, 523
- Ferrarese, L., Merritt, D. 2000, ApJ, 539, L9
- Gebhardt, K., et al. 2000, ApJ, 539, L13
- Graham, A. W., et al. 2001, ApJ, 563, L11
- Houghton, R., et al. 2006, MNRAS, 367, 2
- Laine, S., et al. 2003, AJ, 125, 478
- Magorrian, J., et al. 1998, AJ, 115, 2285
- Marconi, A., Hunt, L. K. 2003, ApJ, 589, L21
- Sarzi, M., et al. 2001, ApJ, 550, 65
- Shapiro, K. L., et al. 2006, MNRAS, 370, 559
- von der Linden, A., et al. 2007, MNRAS in press